REPORT DOCUMENTATION PAGE #31

Form Approved
OMB No. 0704-0188

1. AGENCY USE ONLY *(Leave blank)*

2. REPORT DATE
22 Sept., 1997

3. REPORT TYPE AND DATES COVERED
Final (04/01/95-03/31/97)

4. TITLE AND SUBTITLE
Breakdown of trailing vortices in compressible flows past wings and conical bodies

5. FUNDING NUMBERS
Grant no.F49620-95-1-0302

6. AUTHOR(S)
Fazle Hussain

AFOSR-TR-97
0500

7. PERFORMING ORGANIZATION NAME(S) AND ADDRESS(ES)
Institute for Fluid Dynamics and Turbulence
University of Houston
4800 Calhoun, Houston, TX 77204

9. SPONSORING / MONITORING AGENCY NAME(S) AND ADDRESS(ES)
U.S. Air Force Office of Scientific Research
110 Duncan Avenue Suite B115
Bolling AFB DC 20332-0001

NA

10. SPONSORING / MONITORING AGENCY REPORT NUMBER
F49620-95-1-0302

11. SUPPLEMENTARY NOTES

12a. DISTRIBUTION / AVAILABILITY STATEMENT
unlimited

12b. DISTRIBUTION CODE

13. ABSTRACT *(Maximum 200 words)*

Development of a finite volume code for spatially evolving simulations of flow past wings:

We have developed a three-dimensional finite volume code for performing simulations of spatially evolving flows. The finite volume technique is preferred due to its flexibility for implementing a variety of realistic and physically relevant boundary conditions e.g. unlike spectral codes this method is not constrained to periodic boundary conditions only and therefore allows simulations of flows past wings with finite spans. The algorithm is formulated with equations written in generalized coordinates which makes this code useful for simulating a wide variety of flows including spatially evolving jets, flows past bluff bodies of different geometries, etc. Also, versatile grid-generation is useful in compressible flows for local grid refinement to resolve shocks.

14. SUBJECT TERMS
Vortices, Breakdown

15. NUMBER OF PAGES
7

16. PRICE CODE

17. SECURITY CLASSIFICATION OF REPORT	18. SECURITY CLASSIFICATION OF THIS PAGE	19. SECURITY CLASSIFICATION OF ABSTRACT	20. LIMITATION OF ABSTRACT

NSN 7540-01-280-5500

Standard Form 298 (Rev 2-89)

Development of a finite volume code for spatially evolving simulations of flow past wings:

We have developed a three-dimensional finite volume code for performing simulations of spatially evolving flows. The finite volume technique is preferred due to its flexibility for implementing a variety of realistic and physically relevant boundary conditions e.g. unlike spectral codes this method is not constrained to periodic boundary conditions only and therefore allows simulations of flows past wings with finite spans. The algorithm is formulated with equations written in generalized coordinates which makes this code useful for simulating a wide variety of flows including spatially evolving jets, flows past bluff bodies of different geometries, etc. Also, versatile grid-generation is useful in compressible flows for local grid refinement to resolve shocks.

Grid generation is performed in a preprocessor routine which generates a body-fitted , three dimensional , orthogonal grid system. The code computes the Cartesian coordinates of grid points in the transformed system and their corresponding scaling factors to be accessed by the main program. This allows versatility in the specification of the inner boundary which could correspond to an airfoil, a cylinder, etc.. The Cartesian system is used in the computational domain, while the generalized system is the physical domain. Once the grid is generated, the Jacobian of the transformation (from the physical domain to the computational domain) is evaluated at every point. From the value of the Jacobian, the scaling factors are calculated. A noniterative method of grid generation using parabolic differential equations is preferred . The advantages of using a set of parabolic equations are:

- Parabolic equations are initial value problems, so grids are generated by a marching algorithm like the hyperbolic grid generation method.
- The parabolic partial differential equations have most properties of the elliptic equations, particularly, the diffusion effect which smoothes out any singularity of the inner boundary condition.
- By employing the marching algorithm, the computational time required is only a very small fraction of that for the elliptic grid generation.

The governing equations are formulated using finite volume discretisation , with velocities and pressure as the primary variables. The velocity and pressure points are distributed over a staggered grid. The algorithm involves a fractional step method (predictor step and corrector step) to stabilize the advective terms. The method involves an explicit evaluation of the velocities in the predictor and corrector stages and an implicit evaluation of the auxiliary pressure. The code is second-order accurate in space and time (the code has been implemented in a manner which allows easy extension to a compact-storage third order Runge-Kutta scheme); a scheme similar to the SMAC method is used for solving the Navier-Stokes equations. We have implemented this algorithm and validated it. Validation cases include two-dimensional flow in a square lid-driven cavity, using a uniformly spaced Cartesian grid. Streamlines, vorticity contours, center-line velocity, peak vorticity, etc. obtained from this simulation were found to be in good agreement with the results in the literature. In Figs. 6,7 we show vorticity contours in a lid-driven flow in a square cavity for two different Reynolds numbers, these compare very well with documented results in the literature.

(In the following, superscripts denote the relevant publication from the list at the end of the report)

A model of turbulent vortex breakdown[1]*:*

We have developed a theory of turbulent vortex breakdown to predict hysteretic jump transitions in recirculatory zones over delta wings and to explain recent experimental observations of conical vortex breakdown. Our approach involves a) Modeling swirling jets by conically similar solutions of the Navier-Stokes equations (Fig. 1 shows the destroyed vortex in spherical coordinates (r,θ,ϕ), curves 3,4 show typical streamlines of the meridional motion in the two flow cells separated by a conical surface), b) modeling turbulence by an eddy viscosity which is represented by a step function of the polar angle and c) matching solutions for the laminar and turbulent flow regions. The model shows the formation of a conical turbulent wake which develops without a recirculatory zone. Fig. 2 shows the results of the these calculations where the velocity at the axis, v_a is plotted as a function of the long parameter, M. This parameter is defined as

$$M = 2\pi J_0 / Re_s^2 ,$$

where, J_0 is a measure of the flow force acting on the plane normal to the axis and Re_s is the Reynolds number of the vortex based on its circulation. The plot shows the velocity on the axis for both turbulent (T) and laminar (L) flows. Positive values of v_a correspond to the consolidated jet and negative values to the two-cell flow. One can see that the curves have folds at smaller values of $M=M_f$ than $M=M_s$ for flow separation ($v_a=0$). The results obtained for the laminar flow coincide with those obtained by Long. Our results also provide upper estimates for the angles of the conical wake region where the turbulence is strong and for the vortex core where the swirl is of the solid body type. The prediction of the conical wake and the estimates for its angle also agree with earlier studies.

Vortex breakdown control using vortex generators[2]*:*

To develop effective means to control vortex breakdown in wing-tip and leading edge vortices, we have studied swirling flows in a confined cylinder. Such a confined flow is relevant to the study of this problem as it is free from ambient disturbances. The basic flow is driven by a rotating disc and is characterized by a Reynolds number, Re_D. A thin vortex core, which develops at the axis at large Re_D, undergoes breakdown. The core is the most sensitive flow region and is forced by an independently rotating rod (with Reynolds number, $Re_\tau \sim Re_D / 100$) which has a diameter comparable to that of the core. Flow visualization revealed that even weak forcing by the rod can strongly influence the flow (Fig. 3). With increasing rod co-rotational speed, the size of the breakdown 'bubbles' decreases and eventually a conical wake without any recirculating regions is formed. In contrast, when the rod is counter-rotated, the number and size of the bubbles increases (Fig. 4). We have developed a theoretical model to explain the physics of these flow pattern transformations. We have found that the flow with a co-rotating rod can be modeled using conically similar solutions of the Navier-Stokes equations. Fig. 5 shows the modeled shape of the wake when vortex breakdown is suppressed which closely corresponds to the wake surface observed via flow visualization.

Inviscid Vortex Breakdown[5]*:*

We demonstrated that axisymmetric vortex breakdown in a steady flow in a semi-infinite circular pipe is a reversible process which appears due to solution nonuniqueness in some range of inflow parameters, when the entire flow jumps to another metastable steady state with the same boundary conditions. All such solutions are smooth along the pipe length and have the same mechanical energy, but the flow forces in the different flow states are different. Vortex Breakdown must appear by continuous change in flow parameters (usually the swirl number) when locally the solution fails to exist because of fold or similar catastrophe which can be related to transcritical bifurcation of a degenerate state (characterized by the existence of trivial solutions), but the spontaneous jumps between different solutions (not on a fold) also are considered as a finite perturbation instability. Among the possible ways to eliminate degeneracy, we consider the injection of azimuthal vorticity into the vortex core at the pipe entrance. We show that the flow pattern inside the steady near-axis separation zone (usually associated with vortex breakdown) depends on the flow history. Therefore, our approach to vortex breakdown takes into account the flow pattern inside the separation zone. We consider two approaches: the traditional analytic continuation method (leading to a recirculation zone) and the stagnant separation zone model (without velocity jump on its boundary). We reveal serious defects of the analytic continuation method: infinite negative velocity at a finite inflow swirl and global nonexistence of solutions. Analytic continuation can only lead to jump transition from a stable state to an unstable state or internal separation, but not vortex breakdown. The new stagnation zone model is superior in that solutions always exist and, for large enough inflow swirl, exhibit nonuniquenes and folds by smooth variations of the flow parameters, thus predicting the experimentally observed hysteretic jump transitions in vortex breakdown. This model has revealed, in addition, some new phenomena, such as vortex contraction and a 'finite distance' effect: with increasing swirl a stagnation zone of nonzero size suddenly appears far downstream and, consequently, the stagnation zone inside the pipe abruptly arises at a finite distance from the inflow.

Vortex Breakdown as inviscid separation in steady flows[6]:

We studied vortical channel flows with different inflow vorticity distributions and showed that an exactly stagnant separation zone is formed in the limit that the inflow vorticity becomes discontinuous. It is shown that the analytical continuation model applied to irrotational channel flow with a slender vortical core (the planar analog of the Rankine vortex) yields 'vorticity breakdown'—a phenomenon similar to vortex breakdown in swirling flows. This study is related to the classical problem of the indeterminacy of steady, inviscid, incompressible vortical planar flows due to presence of separation. We have proved that any inviscid steady flow is 'totally nonunique' in the sense that there exists a continuum of possible solutions involving recirculation zones which satisfy the same boundary conditions. For sufficiently large inflow vorticity, the formation of separation zones is inevitable. Various additional phenomenological conditions to achieve uniqueness and to determine the flow in the separation zone were evaluated. We revealed a new 'measure paradox': a stagnation zone of finite area arises from one streamline by changing vorticity at only one inflow point. We focus on this new steady stagnant zone with continuous velocity distribution everywhere. The existence and uniqueness theorems for a flow with stagnation zone were proved. We showed that the kinetic energy of the entire flow domain is minimized when the separation zone is stagnant and is completely contained within any possible recirculation zone. Nonuniqueness and hysteresis-related multiple solutions are inherent to those solutions with recirculation zones where very large (physically unrealistic) velocity in the reversed flow appears. Being free from these drawbacks, the stagnation zone model appears to be superior. A numerical investigation of a time-evolving vortical flow in a square domain confirmed the existence of a critical value of inflow vorticity, above which the flow is unsteady, depending on the initial condition within the domain.

Hysteresis in swirling jets[3]:

Vortex breakdown can be viewed as a hysteretic transformation in swirling jet. We consider viscous flows with steady rotationally symmetric motion above an infinite conical stream surface with a half-angle, θ_c. The flows analyzed are generalizations of Long's vortex. They correspond to conically similar solutions of the Navier-Stokes equations and are characterized by circulation, Γ_c given at the surface and axial force J_1. Asymptotic analysis and numerical computations show that four (for $\theta_c \leq 90°$) or five ($\theta_c >$ $90°$) solutions exist in some range of Γ_c and J_1. The solution branches form hysteresis loops which are related to jump transitions between various flow regimes. Four kinds of jumps were found: (i) vortex breakdown which transforms a near-axis jet into a two-cell flow with reverse flow near the axis and an annular jet fanning out along conical surface $\theta = \theta_s < \theta_c$; (ii) vortex consolidation causing a reversal of (i); (iii) jump flow separation from surface $\theta = \theta_c$; and (iv) jump attachment of the swirling jet to the surface. As Γ_c and / or J_1 decrease, the hysteresis loops disappear through a cusp catastrophe. In particular, vortex breakdown can be interpreted as a fold catastrophe. Two new and striking effects were found: (i) there is a pressure peak of $O(\Gamma_c^2)$ inside the annular swirling jet; and (ii) a consolidated swirling jet forms with a reversed ('anti-rocket') flow force.

Publications

1. V. Shtern, M. Herrada and F. Hussain, 1997, A model of turbulent vortex breakdown, 4th AIAA Shear Flow Conference, Snowmass, CO, June 30-July 2, 1997, *AIAA 97-1842*
2. H. Husain, V. Shtern and F. Hussain, 1997, Control of vortex breakdown using vortex generators, 4th AIAA Shear Flow Conference, Snowmass, CO, June 30-July 2, 1997, *AIAA 97-1879*
3. V. Shtern and F. Hussain, Hysteresis in swirling jets, 1996, *J. Fluid Mech.*, **309**, p. 1
4. V. Shtern, A. Borissov and F. Hussain, Vortex sinks with axial flow: solution and applications, 1997, *Phys. Fluids*, **9** (10)
5. M. Goldshtik and F. Hussain, Inviscid vortex breakdown, (in preperation.)
6. M. Goldshtik and F. Hussain, Inviscid separation in steady planar flows, (in preperation.)

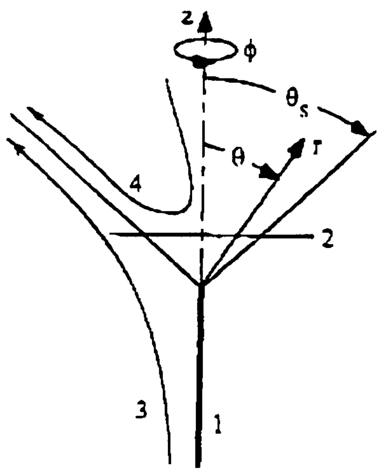

Fig 1: Schematic of the problem and the coordinates

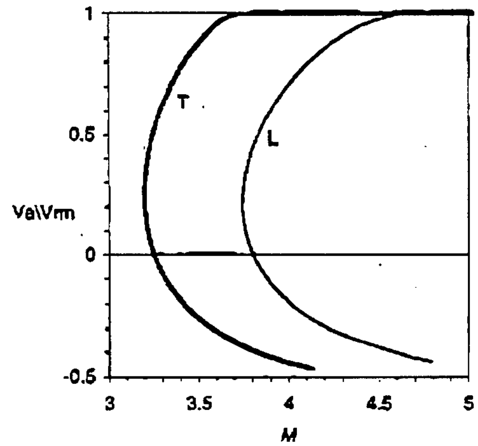

Fig 2: Fold catastrophe in the laminar (L) and turbulent (T) flows

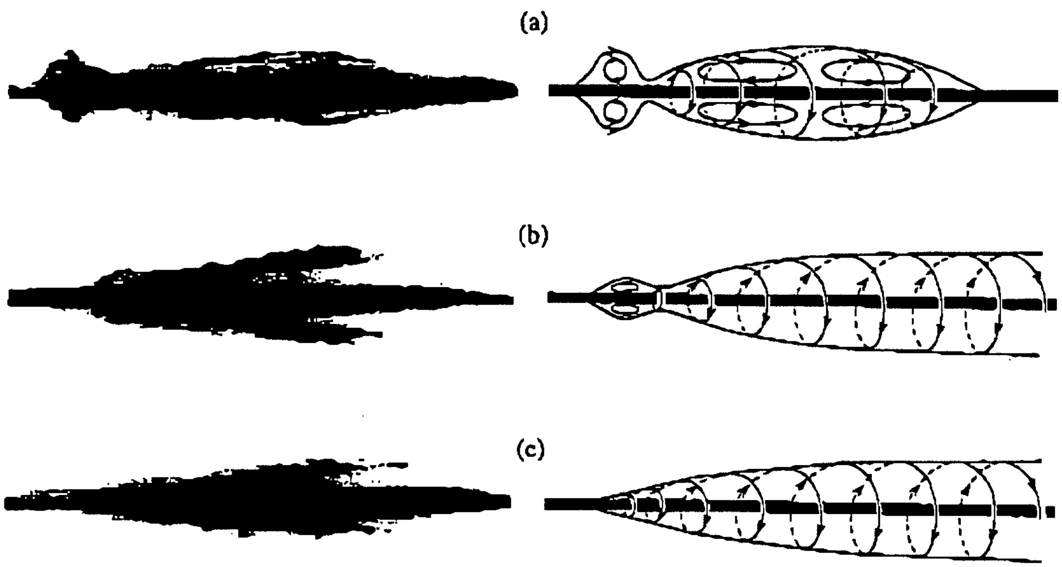

Fig. 3: Flow visualization pictures and schematics of streaklines for co-rotating disc and central rod. Re_d=2720. (a) Re_r=0; (b) Re_r=21; (c) Re_r=29. Arrows in the schematics indicate flow direction.

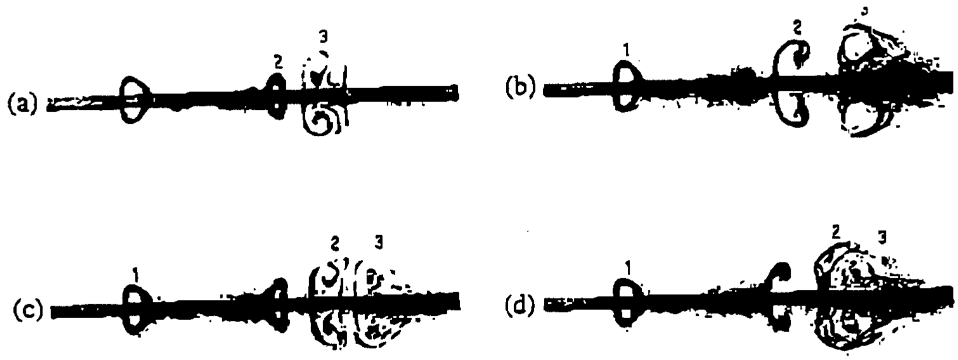

Fig 4: Flow visualization pictures showing time evolution of multiple vortex breakdown bubbles for the case of counter-rotating disc and central rod. Re_d= 2720, Re_r=14.5.

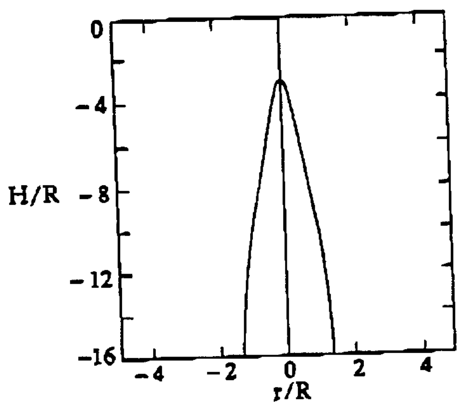

Fig. 5: Analytical solution for the shape of the conical wake observed in the case of co-rotating disc and rod.

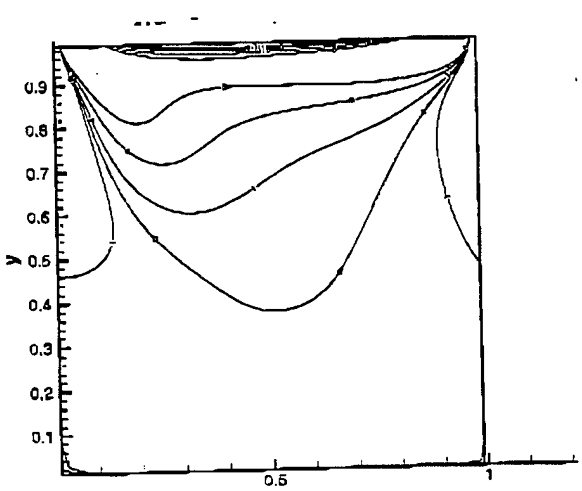

Fig. 6: Vorticity contours in a lid-driven cavity flow at Re=100; t=1.5

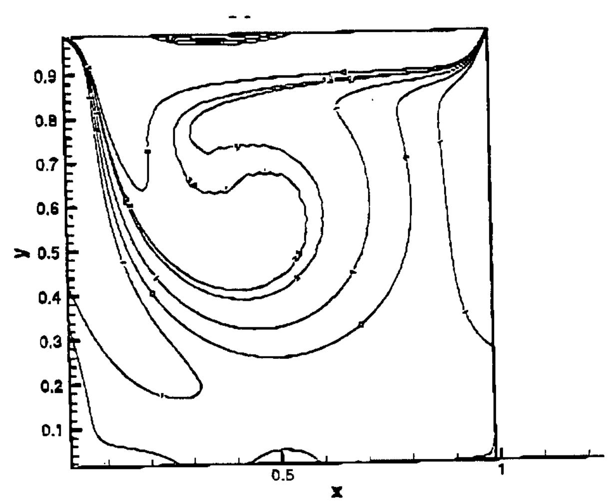

Fig. 7: Vorticity contours in a lid-driven cavity flow at Re=400; t=9